China Ocean Eng., 2018, Vol. 32, No. 4, P. 422–430
DOI: https://doi.org/10.1007/s13344-018-0044-7, ISSN 0890-5487
http://www.chinaoceanengin.cn/ E-mail: coe@nhri.cn

Dynamic Performance Analysis of the Tuned Heave Plate System for Semi-Submersible Platform

LIANG Hai-zhi[a, b], LIU Kun[c, *], LI Lu-yu[b], OU Jin-ping[b]

[a]School of Civil Engineering, Qingdao University of Technology, Qingdao 266033, China

[b]State Key Laboratory of Coastal and Offshore Engineering, Dalian University of Technology, Dalian 116024, China

[c]School of Civil and Transportation Engineering, South China University of Technology, Guangzhou 510640, China

Received December 14, 2017; revised April 18, 2018; accepted May 22, 2018

Abstract

Logistical supply is costly for the deepwater oil and gas exploitation, thereby it is necessary to develop a novel power supply solution to improve the offshore structure's self-holding capacity. The two-body point absorbers, as a renewable energy device, have achieved a rapid development. Heave plate is used to constrain the truss's motion in the two-body point absorber, and the floater moves along the truss up and down. This two-body point absorber can be considered to be an essentially mass-spring-damper system. And it is well known that the heave plates have been widely used in the Spar platform to suppress the heave motions. So if the two-body point absorber can be modified to combine with offshore floating structures, this system can not only offer electric power to support operations or daily lives for the platform, but also control the large motions in the vertical plane. Following this concept, a novel tuned heave plate (THP) system is proposed for the conventional semi-submersible platform. In order to investigate the dynamic performances of the single THP, two experiments are conducted in this paper. First, the hydrodynamic coefficients of the heave plates are studied, and then the THP experiments are carried out to analyze its dynamic performance. It can be concluded that this THP is feasible and achieves the design objective.

Key words: tuned heave plate, hydrodynamics, wave energy conversion, dynamic performance

Citation: Liang, H. Z., Liu, K., Li, L. Y., Ou, J. P., 2018. Dynamic performance analysis of the tuned heave plate system for semi-submersible platform. China Ocean Eng., 32(4): 422–430, doi: https://doi.org/10.1007/s13344-018-0044-7

1 Introduction

For the offshore oil and gas exploitation industry, it is more urgent to have an efficient and reliable offshore equipment to reduce the production cost. Top tensioned riser with dry tree, allowing to drill, complete, and work over a well directly from the same platform, is cost-effective for subsea intervention. The dry tree system is widely utilized by the tension leg platforms (TLPs) and Spars, due to their excellent heave performance. However, the TLP will be cost prohibitive in the ultra-deep water and Spar is limited by its small variable deck load. Semi-submersible platform is an economical solution for offshore drilling, production, pipe laying and other deep-water applications. The shortcoming of semi-submersible is that it is susceptible to large heave motions under wave loading and therefore a dry-tree oil production system is not feasible.

The deepwater offshore floating structures generally work in remote ocean locations, and the logistics are costly. If a novel power supply solution is provided for the operations, the self-holding capacities of the offshore structures will be further enhanced. Wave energy convertor (WEC) is one of the attractable solutions for the conventional floating structure to supply power (Kathleen and Edwards, 2014).

WEC systems can be divided into several types according to the energy conversion principles, such as point absorber, oscillating water column (OWC), and pitching. The point absorber harvests the wave energy from the float heave motions. In the OWC, a bidirectional turbine is driven to convert wave power by the air which is compressed or decompressed by the wave elevation. The floating-pitching device converts wave energy from its pitching motion. By Comparing the styles of these three devices, it can be found that it is possible to convert the kinetic energy of the heave DOF of the floating structures into the electrical power by the point absorber.

PowerBuoy designed by Ocean Power Technologies consists of a floater, a power take-off system (PTO), truss and a heave plate as shown in Fig. 1 (OPT, 2016). The en-

Foundation item: This work was financially supported by the Fundamental Research Program of Shandong Province (Grant No. ZR2016EEQ23), and the Youth Exploration Project of Shandong Province Mount Tai Scholar Advanced Disciplinary Talent Group.

*Corresponding author. E-mail: kunliu_hit@hotmail.com

ergy is generated from the electro-hydraulic device due to the relative wave excited motions between two bodies of the draft floater and heave plate. Therefore, PowerBuoy is known as a two-body point absorber. The electro-hydraulic device can be considered to be a damping element and a pneumatic spring element, which is equivalent to the mass-spring-damper system in essence as shown in Fig. 2. The operating mechanism of the PTO in PowerBuoy is the same as the eddy current tuned mass damper (TMD) (Wang and Chen, 2013) for the civil structures. And the heave plate used to maintain the truss motion is similar to the mass-block of the TMD (de Falcão, 2010; Olaya et al., 2013, 2014).

Heave plates also have been widely used for the Spar platform to suppress the heave motions, and then the efficient top tensioned risers (TTRs) with dry trees can be used (Tao and Cai, 2004). However, the Spar designs require costly and risky topsides installation offshore compared with the semi-submersible platform. Although the natural period of the semi-submersible platform in the heave is designed beyond the range of wave periods, it is not sufficient to support the dry tree riser system. A dry tree semi-submersible platform (Murray et al., 2007) is an alternative solution. Chakrabarti et al. (2007) designed a truss pontoon semi-submersible platform with eight heave plates to improve dynamic performance. Halkyard et al. (2002) designed a deep draft semi-submersible with a retractable heave plate. In these designs, the heave plates offer the added mass and the viscous damping to reduce heave motion for the floater.

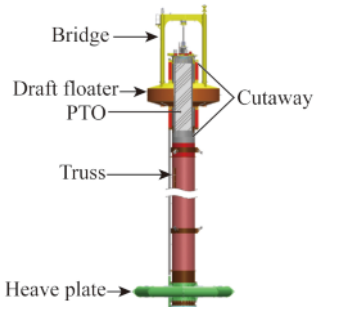

Fig. 1. Schematic of PowerBuoy.

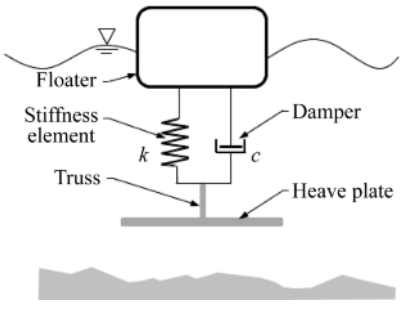

Fig. 2. Mechanism diagram of the mass-spring-damper system.

If the hard connection between the floater and the heave plates in the dry tree semi-submersible platform is replaced by the PTO, the resonance damping can not only supply the power for the operation, but also play an important role in controlling the response heave motion. Following this concept, a tuned heave plates system (THP) is proposed for the semi-submersible platform in this paper. In order to investigate the dynamic performance of the semi-submersible platform with the THP, the subsystem tests of the THP are carried out. The key component in the THP is the heave plate whose hydrodynamics have been studied by Chua et al. (2005), Tao and Dray (2008), Molin (2001), An and Faltinsen (2013). The main contribution of this paper is to analyze the dynamic performance of the THP which is sensitive to the hydrodynamic parameters and tuning frequency. Therefore, the hydrodynamics of the heave plate is studied primarily.

This paper is organized as follows: Both mathematical models of the conventional heave plate and the THP system for the platform are depicted in Section 2. Section 3 describes the experimental setup, and the results are discussed in Section 4. Finally, Section 5 concludes the study.

2 Mathematical model of the THP

2.1 Generic concept of the tuned heave plate

The conceptual design of the THP for the semi-submersible platform equipped with the dynamic positioning system is given in Fig. 3a, and four THPs are installed in the

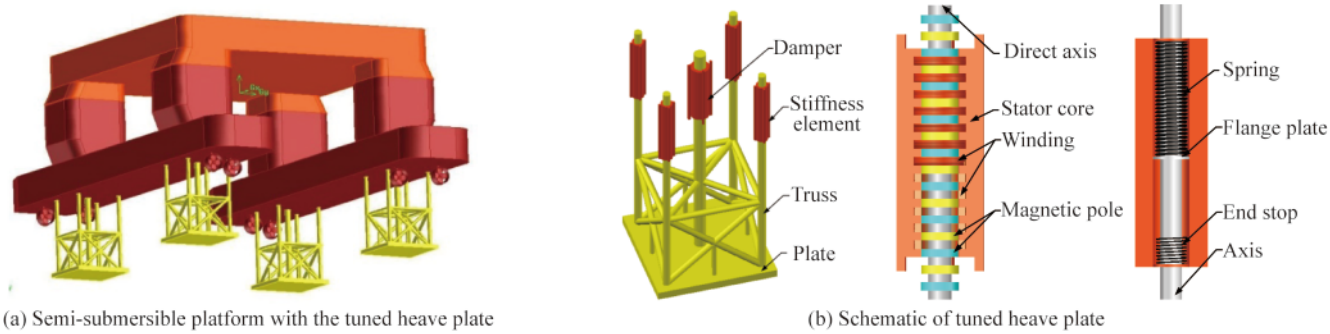

(a) Semi-submersible platform with the tuned heave plate

(b) Schematic of tuned heave plate

Fig. 3. Concept design of the semi-submersible platform with the tuned heave plate.

columns and below the platform's pontoon. The details of the THP are shown in Fig. 3b, and the PTO system includes four stiffness elements and one damper which are all fixed in the column. The damper represents the generators here. Unlike the truss pontoon semi-submersible platform with a large size heave plate, the smaller size plate for the THP is convenient to be installed and this multi-THP system can also achieve the anti-roll control objective as the multi-TMD system (Li, 2000). The remarkable plate added mass is beneficial for the THP to obtain an ideal mass ratio. However, the plate drag viscous damping from the fluid is very complex and makes the THP dynamic response uncertain. Therefore, it is necessary to study the dynamic performance of the single tuned heave plate.

2.2 Conventional heave plate mathematical model

The hydrodynamic force acting on the heave plate can be described by the Morrison equation (Tao and Dray, 2008), as:

$$F(t)=\rho\nabla C_{\mathrm{a}}\ddot{\boldsymbol{x}}+\frac{1}{2}\rho AC_{\mathrm{d}}\dot{\boldsymbol{x}}|\dot{\boldsymbol{x}}|, \tag{1}$$

where C_{a} is the added mass coefficient, C_{d} is the drag coefficient, ∇ is the equivalent volume of water displaced, $\nabla=AL$, L and A are the plate width and project area, and ρ is the density of water.

The plate hydrodynamic parameters C_{a} and C_{d} depend on the Keulegan-Carpenter number (KC) and frequency parameter β which are determined by the motion amplitude a and frequency f as:

$$KC=\frac{2\pi a}{L},\ \beta=\frac{D^2 f}{\mu}, \tag{2}$$

where μ is the kinematic viscosity of the fluid. And then, the Reynolds number can be obtained based on KC and β, as:

$$Re=(KC)\cdot\beta=\frac{a\omega D}{\mu}, \tag{3}$$

where ω is the circular frequency, and $\omega=2\pi f$. When the time history of force $F(t)$ is measured, the coefficients of the damping and added mass can be calculated by using the least square fitting method based on Eq. (1).

2.3 Tuned heave plate mathematical model

When the semi-submersible platform assembles the THP, each THP force acting on the floater according to the mechanism as the mass-spring-damper system in Fig. 2 is given by

$$F_{\mathrm{PTO}}=-c\dot{z}_{\mathrm{rel}}-kz_{\mathrm{rel}}, \tag{4}$$

where $\dot{z}_{\mathrm{rel}}$ and z_{rel} are the relative velocity and motion between the platform and the heave plate, k is the stiffness coefficient of stiffness element and c is the damping coefficient of the damper. The control performance of the THP is determined by the reacting force F_{PTO}, and the energy harvesting capability depends on the damping term $c\dot{z}_{\mathrm{rel}}$. The mathematical model of the semi-submersible platform with the THP is built based on the Cummins equation (Cummins, 1962)

$$\left(\boldsymbol{m}^F+\boldsymbol{m}_{\mathrm{a}}^F\right)\ddot{\boldsymbol{x}}(t)+\int_{-\infty}^{t}\dot{\boldsymbol{x}}\boldsymbol{K}(t-\tau)\mathrm{d}\tau+\boldsymbol{C}_F\dot{\boldsymbol{x}}(t)+\boldsymbol{K}_F\boldsymbol{x}(t)=\boldsymbol{F}_{\mathrm{Dis}}+\boldsymbol{H}_1\boldsymbol{F}_{\mathrm{DP}}-\boldsymbol{H}_2\boldsymbol{F}_{\mathrm{PTO}}, \tag{5}$$

where $\ddot{\boldsymbol{x}}$, $\dot{\boldsymbol{x}}$ and $\boldsymbol{x}$ are the platform acceleration, velocity and displacement vectors; $\boldsymbol{m}^F$ and $\boldsymbol{m}_{\mathrm{a}}^F$ are the matrices of the platform mass and added mass; $\boldsymbol{K}$ is the retardation function; $\boldsymbol{C}_F$ is the linear viscous damping matrix; $\boldsymbol{K}_F$ is the hydrodynamic stiffness matrix; $\boldsymbol{F}_{\mathrm{Dis}}$ is the external disturbance including wave, wind and current forces; $\boldsymbol{F}_{\mathrm{DP}}$ is the dynamic positioning control force; and $\boldsymbol{H}_1$ and $\boldsymbol{H}_2$ are the corresponding transfer matrices of $\boldsymbol{F}_{\mathrm{DP}}$ and $\boldsymbol{F}_{\mathrm{THP}}$.

$$\boldsymbol{H}_1=\begin{bmatrix}1&0&0&0&0&0\\0&1&0&0&0&0\\0&0&0&0&0&1\end{bmatrix}^{\mathrm{T}};$$

$$\boldsymbol{H}_2=\begin{bmatrix}0&0&1&l_{y,1}&-l_{x,1}&0\\0&0&1&l_{y,2}&-l_{x,2}&0\\0&0&1&l_{y,3}&-l_{x,3}&0\\0&0&1&l_{y,4}&-l_{x,4}&0\end{bmatrix}^{\mathrm{T}},$$

where $[l_{x,i}\ l_{y,i}]$ is the location coordinate of the i-th THP in the horizontal plane. $\boldsymbol{F}_{\mathrm{PTO}}$ is

$$\boldsymbol{F}_{\mathrm{PTO}}=-\boldsymbol{c}\dot{\boldsymbol{x}}_{\mathrm{THP}}-\boldsymbol{k}\boldsymbol{x}_{\mathrm{THP}}, \tag{6}$$

where $\dot{\boldsymbol{x}}_{\mathrm{THP}}$ and $\boldsymbol{x}_{\mathrm{THP}}$ are the relative velocity and displacement vectors of the THP to the semi-submersible platform. By further considering the Morison force of the heave plate (Eq. (1)), the mathematical model of the i-th THP based on the Newton second law is built as:

$$\left(\rho\nabla C_{\mathrm{a}}+m_{\mathrm{p}}\right)\ddot{x}'_{\mathrm{THP},i}+\frac{1}{2}\rho AC_{\mathrm{d}}\dot{x}'_{\mathrm{THP},i}\left|\dot{x}'_{\mathrm{THP},i}\right|=F_{\mathrm{PTO},i},\quad i=1,2,...,4 \tag{7}$$

where m_{p} is the dry mass of the plate; $\ddot{x}'_{\mathrm{THP},i}$ and $\dot{x}'_{\mathrm{THP},i}$ are the total velocity and acceleration of the heave plate in the body-fixed frame. The plate is far away from the free surface, and then the wave force acting on the plate is much smaller than the Morison force such that it can be neglected. In order to avoid the spring with a large initial tensile deformation by the THP's deadweight, the plate is designed to have small density or a suitable thickness to have enough buoyancy to resist its own weight.

3 Experimental setup

The dynamic performance of the tuned heave plate is investigated through the forced oscillation experiment in this section. The experiments were carried out in the nonlinear wave flume at the State Key Laboratory of Coastal and Offshore Engineering of Dalian University of Technology. The wave flume is 60.0 m in length, 4.0 m in width and 2.5 m in depth.

The schematic of the experimental setup is shown in Fig. 4. A servo drive system consisting of an AC servo motor and ball screw etc. is used to simulate the platform's mo-

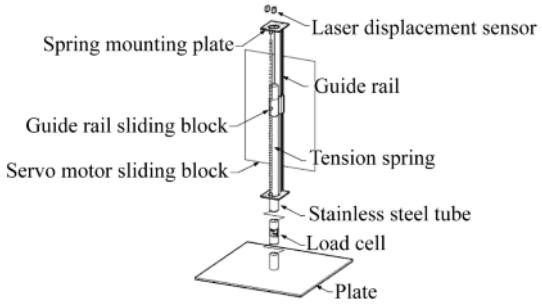

Fig. 4. Experimental setup schematic of the tuned heave plate system.

tion. In order to make sure that the plate can oscillate in the vertical direction, the guide rail is attached to the leadscrew nut. The heave plate is assembled with the guide rail sliding block through the rigid tube. Two spring mounting plates are welded to each end of the guide rail, and then they are connected to the guide rail sliding block by the tension springs.

A load cell is used to measure the hydrodynamic force from the heave plate. In addition, the displacements of the heave plate and the servo motor's excitation are recorded by two laser displacement sensors installed at the top of the system. The experiments in this paper focus on the effects of the heave plate hydrodynamics on the THP's dynamic performance, thus, the damper element is not taken into account in this stage. Fig. 5 is the photograph of the experimental setup.

Two tests are carried out in this study, separately. First, the hydrodynamic performance of the heave plate is studied. The guide rail sliding block is locked, and the plate is forced

Fig. 5. Experimental setup of the tuned heave plate system.

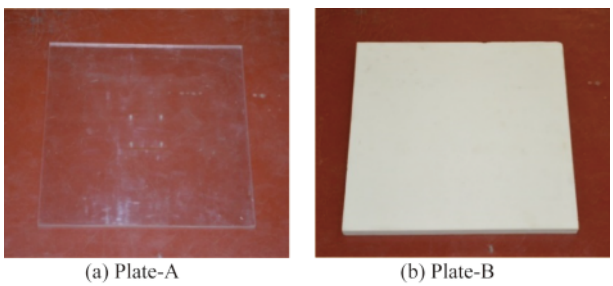

(a) Plate-A (b) Plate-B

Fig. 6. Heave plates used in the experiments.

Table 1 Material and dimensions of the heave plates

	Plate-A	Plate-B
Material	Acrylic	Rigid polyurethane foam
Length (mm)	400	400
Width (mm)	400	400
Thickness (mm)	10	30

to oscillate under the given excitation. Two square plates with different thicknesses shown in Fig. 6 are adopted, and their dimensions are given in Table 1. Plate-A is used to verify the feasibility of the experimental devices. Plate-B made by small density rigid polyurethane foam is thicker than Plate-A, thus, the buoyancy of Plate-B can resist the upper structure's deadweight and keep the spring deformation at a reasonable range. Plate-B's hydrodynamics are also investigated to analyze the effect of the plate thickness. The second test is the tuned heave plate test which is carried out to assess the system's dynamic performance.

4 Result analyses

4.1 Hydrodynamics of the conventional heave plate

From the experimental schematic in Fig. 5, it can be seen that the forces recorded by the load cell include the Morrison force of the heave plate, the hydrostatic stiffness force due to the free surface and the inertia force of the structure, and all these forces are written as:

$$F_{\mathrm{LC}} = (M + \rho V C_{\mathrm{a}})\ddot{\boldsymbol{x}} + \frac{1}{2}\rho A C_{\mathrm{d}} |\dot{\boldsymbol{x}}| \dot{\boldsymbol{x}} + k_{\mathrm{fr}} \boldsymbol{x}, \tag{8}$$

where M is the total dry mass of the plate and tube below the load cell, k_{fr} is the hydrostatic stiffness coefficient of the tube. Therefore, compared with the heave plate Morison equation Eq. (1), the inertia force of the devices and the hydrostatic stiffness force in Eq. (8) should be subtracted to calculate the plate inertia and drag force. When the modified Morison force is obtained, the least squared method is used to fit the added mass coefficient C_{a} and the drag coefficient C_{d}.

The immersed water depth is 500 mm, two oscillation periods are adopted, at 5000 ms and 10000 ms, and the excitation amplitudes are ranged from 20 mm to 100 mm in Test-1. The KC number varied over the excitation amplitude rang. At least 15 cycle motions and forces sampled at a frequency of 50 Hz are recorded in each test. One typical period time history of Plate-A's displacements is shown in Fig. 7, and Fig. 8 shows the corresponding forces. The excitation period is 5 s, and the amplitude is 100 mm. The velocity and acceleration are determined by the numerical derivation. It is inevitable that there will be noise in the recorded signal. In order to make sure no phase lag is introduced, the initial signal is filtered by using the Smooth function in the Matlab toolbox.

The inertia forces, damping forces and hydrodynamic force shown in Fig.9, are obtained by using the fitting coef-

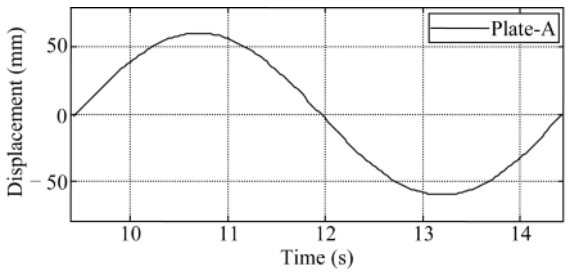

Fig. 7. Time history of Plate-A's displacements.

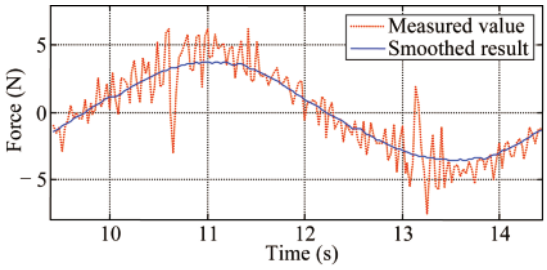

Fig. 8. Time history of Plate-A's forces.

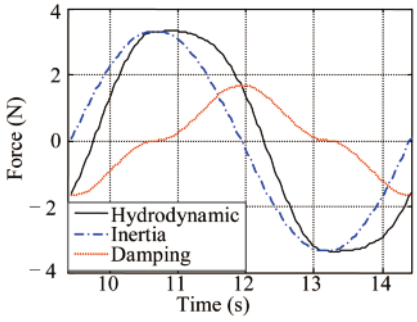

Fig. 9. Time history of Plate-A's forces.

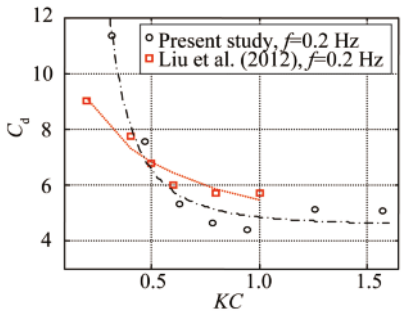

Fig. 10. Drag coefficients of Plate-A.

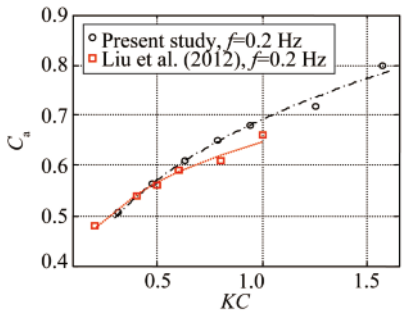

Fig. 11. Added mass coefficients of Plate-A.

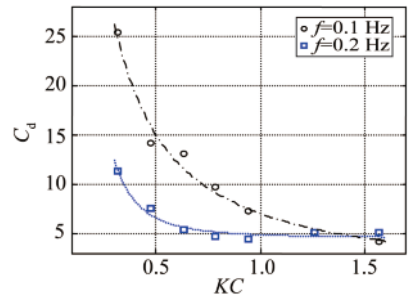

Fig. 12. Effects of the oscillation frequencies for the drag coefficients.

ficients C_a and C_d. The damping coefficient C_d and the added mass coefficient C_a of Plate-A over the various KC numbers under 0.2 Hz oscillation frequency are shown in Figs. 10 and 11. It can be seen that the added mass coefficient C_a is consistent with the literature results of Liu et al. (2012). The value of C_a rises with the increasing KC number. The drag coefficient C_d is much more sensitive to the KC number, especially when the KC number is smaller than 0.5. The trend of C_d is to exponentially decline with KC. And C_d tends to be constant for the KC number larger than 0.6. And this result is similar to the result of Liu et al. (2012).

The effects of the oscillation frequency for C_a and C_d of Plate-A are investigated in Figs. 12 and 13, respectively. It can be seen that C_d decreases with the increasing frequency for the same KC number. The reason is that C_d strongly depends on the Reynolds number, but C_d tends to be constant for the large Reynolds numbers, which is consistent with results of Prislin et al. (1998). The overall trend of C_a increases with the increasing frequency. From the results analysis, it can be seen that this experimental device is feasible.

As mentioned previously, the heave plate in THP should be designed to have enough buoyance to resist its own weight. Thus, the rigid polyurethane foam plate is used to make the heave plate in THP. The experiment parameters of Plate-B are given in Table 2. Five oscillation periods, ranging from 3000 ms to 7500 ms, are used, and the amplitudes are from 20 mm to 100 mm. The time history of the displacements with the amplitude of 60 mm at a period of 3 s is shown in Fig. 14, and the corresponding forces are shown in Fig. 15.

The noise in the signal is unavoidable, especially near the peaks and troughs, where there are impulse forces which are produced due to the inertia of the structure below the load cell. And the peak of these forces is much larger than that of Plate-A. These impulse forces are filtered by the Smooth function.

The results of the drag coefficients C_d and added mass

Table 2 Experimental parameters of Plate-B

Water depth (mm)	Period (ms)	Amplitude (mm)	*KC*
500	3000	20	0.3118
	3750	40	0.6236
	5000	50	0.7796
	6250	60	0.9355
	7500	80	1.2473
		100	1.5591

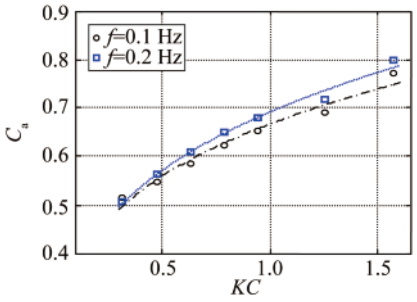

Fig. 13. Effects of the oscillation frequencies for the added mass coefficients.

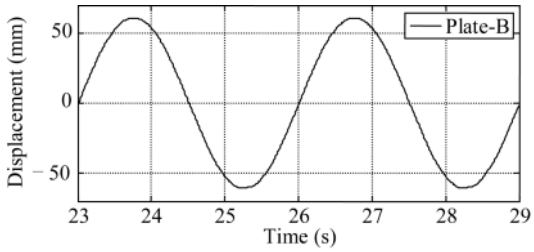

Fig. 14. Time history of Plate-B's displacements.

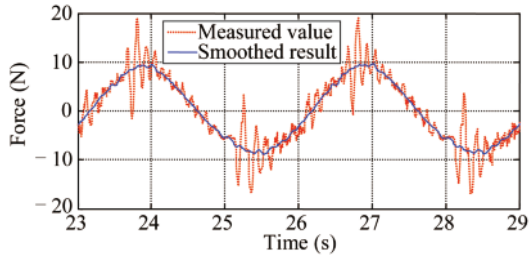

Fig. 15. Time history of Plate-B's forces.

coefficients C_a over *KC* for various excitation frequencies are shown in Fig. 16 and Fig. 17, and the trends are the same as Plate-A. It can be seen that C_d is exponentially declining with *KC* for *KC*<1. For the same *KC* number, C_d decreases with the increasing oscillation frequency. C_a is linear with *KC*, and the added mass coefficient C_a is not sensitive to the oscillation frequency.

The results of C_d and C_a for Plate-A and Plate-B at the frequency of 0.2 Hz oscillation are shown in Fig. 18 and Fig. 19 to analyze the effects of the plate thickness. It can be found that C_d decreases with the increased thickness. These are the same as the results of He et al. (2008), and the damping performance decreases obviously if the thickness to length ratio is larger than 1/50. It also can be seen that C_a of Plate-B is much smaller than that of Plate-A from Fig. 19. This can be attributed to the increased thickness to length ratio, and the motion of Plate-B will make a disturbance to the fluid field and the radiation effect appears.

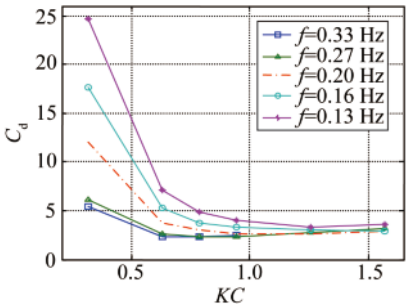

Fig. 16. Drag coefficients of Plate-B.

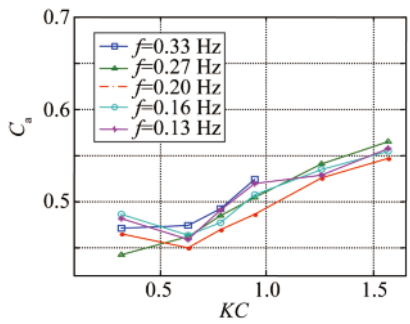

Fig. 17. Added mass coefficients of Plate-B.

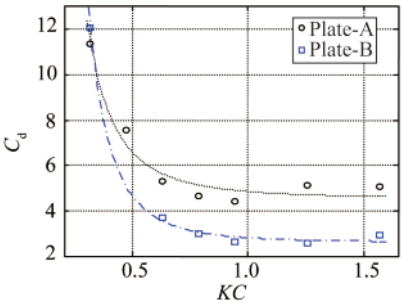

Fig. 18. Effects of the plate thickness on the drag coefficients.

4.2 Tuned heave plate experiment

After the investigation of the plate hydrodynamics, the dynamic performance of the tuned heave plate is studied through the experiment in this section. The length of the prototype plate for the semi-submersible platform is designed to be 17 m. Plate-B is used for the tuned heave plate, and hence the model scale factor is set to be 1:42.5 in the test. The natural period of the semi-submersible platform heave DOF is 19.8 s, and the experimental natural period of the heave DOF is 3.04 s.

The considerable relative motions between the floater

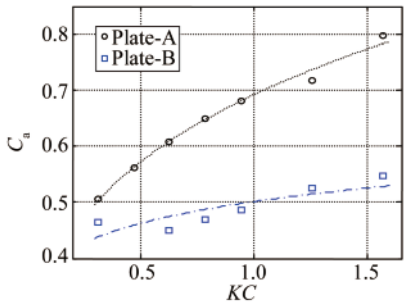

Fig. 19. Effects of the plate thickness on the added mass coefficients.

and heave plate are critical for the wave energy harvest capacity and control performance. In this test, the external damping element has not been considered up to now, and there only exists small friction force generated from the rail sliding block with the rail. The optimal tuning frequency ratio of the THP to the platform's heave DOF is 1 or close to 1. Based on this concept, the natural period of the tuned heave plate system is set to be 3.04 s. The stiffness coefficient of the spring is calculated to be 190.9 N/m based on the fitting added mass coefficient.

Fig. 20 shows the time histories of the actuator and plate displacements. The amplitude and period of actuator are 40 mm and 3 s, respectively. In this case, the frequency ratio of actuator period to the THP's natural period is approximately equal to 1, which is considered that THP is in resonance with the platform's heave DOF motion. It can be found that the motions of the THP are amplified via the tuned system, and the amplitude of the THP is 1.9 times larger than that of the actuator.

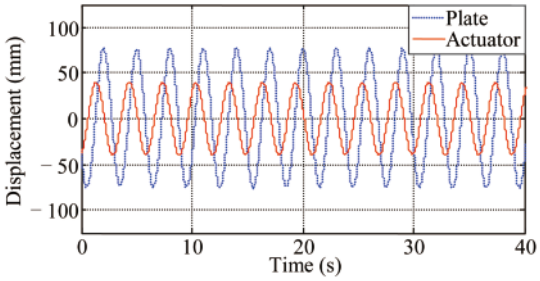

Fig. 20. Time history of the heave plate and actuator displacements.

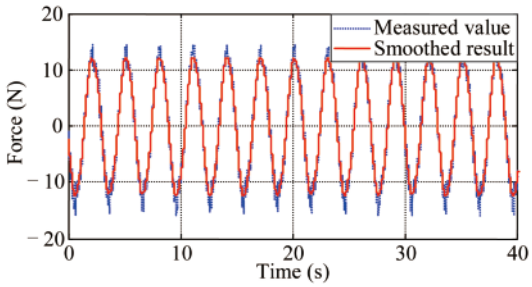

Fig. 21. Time history of the forces acting on the heave plate.

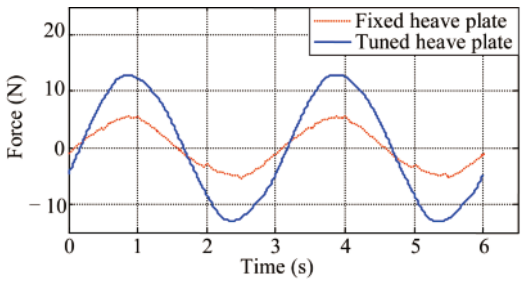

Fig. 22. Time history of the forces acting on the fixed and tuned heave plate.

Fig. 21 gives the time histories of the measured and filtered force from the plate. The forces of the fixed and tuned heave plate are compared under the same excitation condition in Fig. 22. The force amplitude of THP is 2.3 times larger than that of the fixed plate. It can be concluded that the control performance of THP is much better than that of the traditional fixed plate, which is helpful to suppress the platform's heave motions. Amplification coefficient for the movement amplitude of THP is defined to assess the control performance of the THP, as:

$$\beta' = \frac{A_{\text{plate}}}{A_{\text{hull}}}, \tag{9}$$

where A_{plate} and A_{hull} are the movement amplitude of the plate and actuator, respectively.

Fig. 23 shows the amplification coefficients via the excitation periods corresponding to various excitation amplitudes. The peak of the amplification coefficients varied near the platform heave natural period of about 20 s. The reason is that the added mass coefficients of the plates depend on the *KC* number which is related with the oscillation amplitudes. Therefore, for the fixed stiffness coefficient of the spring, the optimal frequency ratio in Fig. 23 is changed with the non-stationary added mass. Meanwhile, the peak values are affected by the viscous damping forces. When the oscillation frequency is smaller than 13 s, the tuning mechanism of the THP is ineffectual anymore. However, there still exists relative motions between the platform and heave plate, and these motions are beneficial

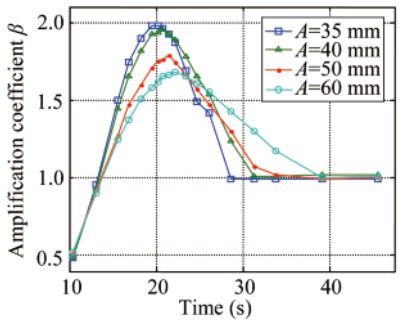

Fig. 23. Displacement amplification coefficients of THP for the heave DOF.

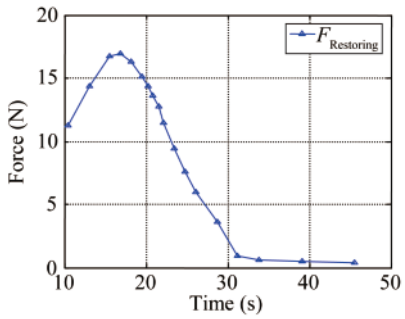

Fig. 24. Resoring force amplitude of THP.

to the energy harvest system. If the oscillation frequency is larger than 28 s, the THP is equivalent with the conventional heave plate.

Based on Eq. (6), the control force acting on the platform is the spring restoring force in this experiment. The restoring force amplitudes under 40 mm oscillation are given in Fig. 24. Compared with the results in Fig. 23, it can be concluded that the considerable restoring force can be obtained from the relative motions. The differences are that when the platform response frequency is smaller than the natural frequency, the heave plate keeps stationary and the platform moves up and down, which is similar to the PowerBuoy. And if the platform response frequencies are larger than 30 s, the platform goes with the large amplitude drift motion, and then the spring effect can be neglected. This situation can be neglected, because it is far away from the wave frequency range and the wave frequency response is very small.

5 Conclusions

The tuned heave plate (THP) system is designed for the semi-submersible platform to convert the platform kinetic energy originated from wave to electric power and improve the platform's dynamic performance in the meanwhile. The hydrodynamic performances of the heave plates are investigated through the experiment. And then, the control performances of THP are certified by using the forced oscillation experiment. From the results, the following conclusions can be obtained.

(1) The drag damping coefficient C_d strongly depends on the *KC* number and shows exponential decline with *KC* number. The value of C_a rises with the increased *KC* number, and it is not very sensitive to the oscillation frequencies compared with C_d.

(2) C_d may decrease with the increased thickness to length ratio. By contrast, C_a is dramatically increased, and the radiation effect should be taken into account.

(3) The feasibility of the THP for the semi-submersible platform is verified through the experimental results. The motions of the heave plate are obviously amplified through the tuned system near the platform's natural period, which is beneficial to improve the platform's dynamic performance. The dry tree riser system becomes a viable option.

(4) The relative motions exist in a wide response frequency range. When the response frequency of the platform is near the natural period, the power is converted from the plate's kinetic energy. And if the response frequency is smaller than 13 s, the platform's kinetic energy is harvested by PTO as PowerBuoy.

The effects of the generator's damping for the THP dynamic performance need to be investigated further, and the control performance should be verified by the platform model experiment in the future.

References

An, S. and Faltinsen, O.M., 2013. An experimental and numerical study of heave added mass and damping of horizontally submerged and perforated rectangular plates, *Journal of Fluids and Structures*, 39, 87–101.

Chakrabarti, S., Barnett, J., Kanchi, H., Meht, A. and Yim, J., 2007. Design analysis of a truss pontoon semi-submersible concept in deep water, *Ocean Engineering*, 34(3–4), 621–629.

Chua, K.H., Clelland, D., Huang, S. and Sworn, A., 2005. Model experiments of hydrodynamic forces on heave plates, *Proceedings of the ASME 2005 24th International Conference on Offshore Mechanics and Arctic Engineering*, Ocean, Offshore and Arctic Engineering Division, Halkidiki, Greece.

Cummins, W.E., 1962. The impulse response function and ship motions, *Schiffstechnik*, 9, 101–109.

de Falcão, A.F.O., 2010. Wave energy utilization: A review of the technologies, *Renewable and Sustainable Energy Reviews*, 14(3), 899–918.

Halkyard, J., Chao, J., Abbott, P., Dagleish, J., Banon, H. and Thiagarajan, K., 2002. A deep draft semisubmersible with a retractable heave plate, *Proceedings of Offshore Technology Conference*, OTC, Houston, Texas, USA.

He, H.P., Troesch, A.W. and Perlin, M., 2008. Hydrodynamics of damping plates at small KC numbers. in: Kreuzer, E. (ed.), *IUTAM Symposium on Fluid-Structure Interaction in Ocean Engineering*, Springer, Dordrecht, Netherlands, pp. 93–104.

Li, C.X., 2000. Performance of multiple tuned mass dampers for attenuating undesirable oscillations of structures under the ground acceleration, *Earthquake Engineering & Structural Dynamics*, 29(9), 1405–1421.

Liu, S.X., Zhao, M., Li, J.X. and Teng, B., 2012. Experimental investigations of hydrodynamic characteristics of the perforated heave plates, *Chinese Journal of Hydrodynamics*, 27(3), 248–255. (in Chinese)

Mekhiche, M.M. and Edwards, K.A., 2014. A renewable energy source for powering offshore oil and gas applications, *Proceedings of the 19th Offshore Symposium*, Texas Section of the Society of Naval Architects and Marine Engineers, Houston, Texas, USA.

Molin, B., 2001. On the added mass and damping of periodic arrays of fully or partially porous disks, *Journal of Fluids and Structures*, 15(2), 275–290.

Murray, J., Tahar, A. and Yang, C.K., 2007. Hydrodynamics of dry tree semisubmersibles, *Proceedings of the 17th International Offshore and Polar Engineering Conference*, International Society of Offshore and Polar Engineers, Lisbon, Portugal.

Olaya, S., Bourgeot, J.M. and Benbouzid, M., 2013. Hydrodynamic coefficients and wave loads for a WEC device in heaving mode,

Proceedings of 2013 MTS/IEEE OCEANS-Bergen, IEEE, Bergen, Norway, 1–8.

Olaya, S., Bourgeot, J.M. and Benbouzid, M., 2014. Modelling and preliminary studies for a self-reacting point absorber WEC, *Proceedings of 2014 International Conference on Green Energy*, IEEE, Sfax, Tunisia, 14–19.

OPT, 2016. *Ocean Power Technologies*, https://www.oceanpowertechnologies.com/powerbuoy/.

Prislin, I., Blevins, R.D. and Halkyard, J.E., 1998. Viscous damping and added mass of solid square plates, *Proceedings of the 17th International Conference on Offshore Mechanics and Arctic Engineering*, ASME, Lisbon, Portugal.

Tao, L.B. and Cai, S.Q., 2004. Heave motion suppression of a Spar with a heave plate, *Ocean Engineering*, 31(5–6), 669–692.

Tao, L.B. and Dray, D., 2008. Hydrodynamic performance of solid and porous heave plates, *Ocean Engineering*, 35(10), 1006–1014.

Wang, Z.H. and Chen, Z.Q., 2013. Development and performance tests of an eddy-current tuned mass damper with permanent magnets, *Journal of Vibration Engineering*, 26(3), 374–379. (in Chinese)